Understanding the properties of the fireball with the polarization signature of thermal dileptons

Florian Seck^{1,*}, Bengt Friman^{2,1}, Tetyana Galatyuk^{2,1}, Hendrik van Hees^{3,4}, Enrico Speranza⁵, Ralf Rapp⁶, and Jochen Wambach¹

Abstract. Multi-differential measurements of dilepton spectra serve as a unique tool to characterize the properties of matter in the interior of the hot and dense fireball created in heavy-ion collisions. An important property of virtual photons is their spin polarization defined in the rest frame of the virtual photon with respect to a chosen quantization axis. Microscopic calculations of in-medium electromagnetic spectral functions have mostly focused on integrated yields which are proportional to the sum of the longitudinal and transverse components of the virtual photon's self-energy, while photon polarization results from the difference of these components. As the processes that drive the medium effects in the spectral function change with invariant mass and momentum, this becomes a powerful tool for studying the medium composition. We present the polarization observables of thermal virtual photons as a function of mass and momentum and confront the results with existing measurements from HADES and NA60.

1 Introduction

Measurements of the electromagnetic (EM) radiation in heavy-ion collisions have provided invaluable information to characterize the strongly interacting matter created in the collision zone. The emission of thermal dileptons with low invariant masses ($M \leq 1$ GeV) mainly originates from the hot and dense hadronic medium with a strongly broadened ρ -meson peak indicating an ultimate melting and transition into a continuum of partonic degrees of freedom [1–4]. Radiation in the intermediate-mass region, $1 \text{ GeV} \leq M \lesssim 3 \text{ GeV}$, has been associated with partonic sources [5] from the early stage of the fireball evolution at temperatures well above the pseudocritical transition temperature obtained from lattice QCD.

The available dilepton world data can successfully be described with spectral functions calculated via hadronic many-body theory, where the predicted melting of the ρ -meson transits into a structureless quark-antiquark $(q\bar{q})$ continuum [6], albeit with substantial enhancements over the free $q\bar{q}$ rate toward low masses constrained by IQCD data [7]. However, the

¹Technische Universität Darmstadt, 64289 Darmstadt, Germany

²GSI Helmholtzzentrum für Schwerionenforschung GmbH, 64291 Darmstadt, Germany

³Institut für Theoretische Physik, Goethe-Universität Frankfurt, 60438 Frankfurt (Main), Germany

⁴Helmholtz Research Academy Hesse for FAIR, Campus Frankfurt, 60438 Frankfurt (Main), Germany

⁵Theoretical Physics Department, CERN, 1211 Geneva 23, Switzerland

⁶Texas A&M University, College Station, TX 77843-3366, USA

^{*}e-mail: f.seck@gsi.de

precise microscopic processes underlying the strongly coupled QCD liquid in the transition regime and deviations caused by non-equilibrium effects remain a matter of debate. Further tests of the existing model calculations including the spin-polarization observables of low-mass dileptons in heavy-ion experiments are therefore desired.

2 Polarization of thermal virtual photons

The rate of thermal dileptons resulting from the EM emissivity of QCD matter is given by

$$\frac{dN_{ll}}{d^4x\,d^4q} = \frac{\alpha^2L(M)}{6\pi^3M^2}f^B(q_0;T)g_{\mu\nu}\varrho^{\mu\nu}_{\rm EM}(M,|\vec{q}|;T,\mu_B) \label{eq:dNll}$$

where $M = \sqrt{q_0^2 - \vec{q}^2}$ denotes the dilepton invariant mass, $f^B(q_0; T)$ the thermal Bose function, α the EM fine-structure constant and L(M) a lepton phase-space factor (L(M)=1) for invariant mass $M \gg m_l$. Using the 4D projectors for a spin-1 particle, $P_{L,T}^{\mu\nu}$, one can decompose the spectral function into its longitudinal and transverse components as [8, 9]

$$\varrho_{\rm FM}^{\mu\nu} = \varrho_L P_L^{\mu\nu} + \varrho_T P_T^{\mu\nu} ,$$

with $g_{\mu\nu}Q_{\rm EM}^{\mu\nu} = \varrho_L + 2\varrho_T$. At zero three-momentum in the heat bath one has $\varrho_T = \varrho_L$, but at finite $|\vec{q}|$ this no longer holds as spherical symmetry is broken.

Angular dependencies in the dilepton production rate can be unraveled by resolving the lepton angle, $\Omega_l = (\phi_l, \theta_l)$, in the photon rest frame [10]. The angular distribution then takes the form

$$\frac{dN_{ll}}{d^4x \, d^4q \, d\Omega_l} \propto \frac{1}{3 + \lambda_{\theta}} \Big(1 + \lambda_{\theta} \cos^2 \theta_l + \lambda_{\phi} \sin^2 \theta_l \cos 2\phi_l + \lambda_{\theta\phi} \sin 2\theta_l \cos \phi_l + \lambda_{\phi}^{\perp} \sin^2 \theta_l \sin 2\phi_l + \lambda_{\theta\phi}^{\perp} \sin 2\theta_l \sin 2\theta_l \sin \phi_l \Big),$$

where the λ 's are the anisotropy coefficients. Even in an isotropic static thermal medium, nontrivial anisotropies in the angular distribution of the produced leptons can occur [10]. The effects are expected to get much larger at smaller masses (M<0.5 GeV), where production processes such as resonance Dalitz decays and Bremsstrahlung contribute and smoothly approach fully transverse polarization at the photon point (M=0 GeV).

Choosing the polarization axis along the photon momentum defines the helicity frame HX'. In the limit of small lepton masses, $m_l \ll M$, the corresponding anisotropy coefficient λ_{θ} is given by

$$\lambda_{\theta}^{\rm HX'}(M,|\vec{q}|) = \frac{\varrho_{\rm T} - \varrho_{\rm L}}{\varrho_{\rm T} + \varrho_{\rm L}} \; , \label{eq:lambda}$$

which highlights its dependence on the *difference* between the polarization components of the EM spectral function. All other anisotropy coefficients vanish as they involve asymmetries with respect to the ϕ_l angle of the leptons. The hadronic spectral function exhibits a non-monotonic dependence of λ_{θ} on the invariant mass as displayed in Fig. 1. By contrast, the polarization of the QGP radiation is rather small, except when approaching the photon point, for $M \lesssim 0.5 \,\text{GeV}$ [11].

In a heavy-ion collision, one generally divides the expanding medium into small cells of locally thermalized matter with medium velocity, $u = \gamma(1, \vec{\beta})$. To compute the polarization of lepton pairs within each cell, the local helicity frame HX' can be reached after a boost into the rest of the medium. The local polarization in the HX' frame, where only $\lambda_{\theta}^{\text{HX'}}$ is finite, needs then to be transformed into a global frame accessible to experiments where all anisotropy

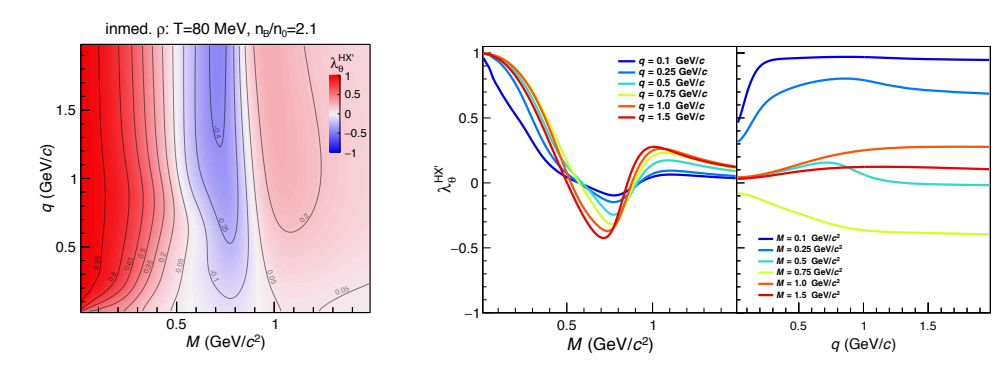


Figure 1. Anisotropy coefficient, $\lambda_{\theta}^{HX'}$ for EM spectral functions in static hadronic matter at T=80 MeV and baryon densities $n_B = 2.1n_0$ (left), together with the corresponding projections of $\lambda_{\theta}^{HX'}$ onto the mass and momentum axis for different momentum and mass bins respectively (right) [11].

coefficients can acquire non-zero values [11, 12]. The helicity (HX) and Collins-Soper (CS) frames are common choices. The resulting polarization observables can then be integrated over all cells and over kinematic variables to match the same mass and momentum window of existing experimental data.

We compare our results to HADES dielectron data [3] measured in Ar(1.76 AGeV)+KCl collisions in the HX frame and NA60 dimuon data [13] from In(158 AGeV)+In collisions in the CS frame, displayed in Fig. 2 for different invariant mass ranges. For the former, the medium evolution is modeled via coarse-grained hadronic transport (UrQMD) simulations, while the collisions at SPS energies are described by an isentropically expanding fireball. The theoretical predictions (red lines) are in good agreement with the data and not far from the functional best fit (blue lines).

The data directly reflect the polarization properties of the hadronic EM spectral function shown in Fig. 1, which exhibits a transition from transverse polarization for masses below 0.5 GeV to a regime where the polarization (integrated over momentum) is small. Thus the near absence of a net polarization (i.e., the rather flat angular distributions) at higher masses is in this calculation not *a priori* related to thermal isotropy arguments.

3 Summary

While dilepton invariant mass and momentum spectra rely on the sum of the transverse and longitudinal components of the spectral function, polarization observables are sensitive to their difference. Virtual photons emitted from dense hadronic matter exhibit a structure where a transverse polarization at low masses transitions into a longitudinal one in the ρ -meson mass region. At high temperatures and smaller baryon densities, these structures become less pronounced and more closely resemble the polarization of QGP emission.

After carrying out the transformations from the local thermal frames into angular variables accessible in the experiment, we find a good agreement between our calculation and data from HADES and NA60, supporting the microscopic description underlying our model.

With future high-rate experiments coming online soon, polarization observables will play an important role in exploring the mechanisms governing the dilepton emission in heavy-ion collisions, e.g., multi-differential measurements of the anisotropy of lepton pairs may help to disentangle the dominant source in the M=1-1.5 GeV region, where "chiral mixing" between the ρ and a_1 channels via πa_1 annihilation competes with $q\bar{q}$ annihilation.

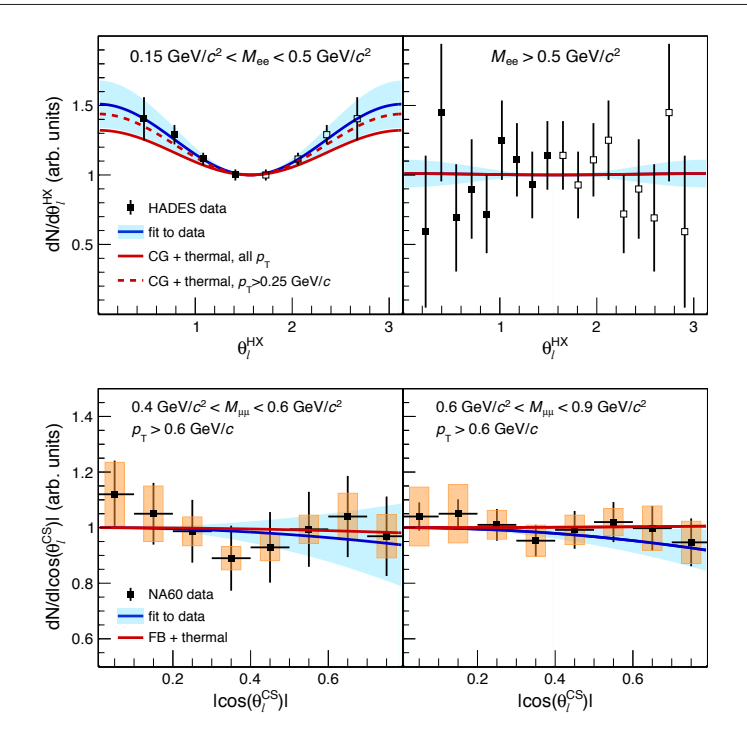


Figure 2. Upper row: comparison of calculated angular distributions (red lines), integrated over two dielectron mass bins, to HADES data in Ar(1.76 AGeV)+KCl collisions [3]. Fits by the HADES collaboration (blue lines with bands) yield anisotropy parameters of λ_{θ} =0.51 ± 0.17 (left) and 0.01 ± 0.1 (right) for the lower and higher mass window, respectively, compared to 0.32 and 0.01 from the present calculations. Lower row: calculated angular distributions (red lines), integrated over two dimuon mass windows, in the CS frame, compared to NA60 data in In(158 AGeV)+In collisions [13]. The blue lines represent fits by NA60 with extracted anisotropy parameters of λ_{θ} = -0.10 ± 0.24 (left) and -0.13 ± 0.12 (right), compared to the calculated values of -0.04 and 0.01, respectively [11].

References

- [1] R. Arnaldi et al. (NA60), Phys. Rev. Lett. 96, 162302 (2006), nucl-ex/0605007
- [2] L. Adamczyk et al. (STAR), Phys. Rev. Lett. 113, 022301 (2014), [Addendum: Phys.Rev.Lett. 113, 049903 (2014)], 1312.7397
- [3] G. Agakishiev et al. (HADES), Phys. Rev. C 84, 014902 (2011), 1103.0876
- [4] J. Adamczewski-Musch et al. (HADES), Nature Phys. 15, 1040 (2019)
- [5] R. Rapp, H. van Hees, Phys. Lett. B **753**, 586 (2016), 1411.4612
- [6] R. Rapp, J. Wambach, Eur. Phys. J. A 6, 415 (1999), hep-ph/9907502
- [7] R. Rapp, Adv. High Energy Phys. **2013**, 148253 (2013), 1304.2309
- [8] L.D. McLerran, T. Toimela, Phys. Rev. D 31, 545 (1985)
- [9] N.P. Landsman, C.G. van Weert, Phys. Rept. 145, 141 (1987)
- [10] E. Speranza, A. Jaiswal, B. Friman, Phys. Lett. B 782, 395 (2018), 1802.02479
- [11] F. Seck, B. Friman, T. Galatyuk, H. van Hees, E. Speranza, R. Rapp, J. Wambach (2023), 2309.03189
- [12] P. Faccioli, C. Lourenço, Particle Polarization in High Energy Physics (Springer, 2022)
- [13] R. Arnaldi et al. (NA60), Phys. Rev. Lett. 102, 222301 (2009), 0812.3100